ORIGINAL ARTICLE

A superconducting joint for GdBa$_2$Cu$_3$O$_{7-\delta}$-coated conductors

Yeonjoo Park[1], Myungwhon Lee[2], Heesung Ann[2], Yoon Hyuck Choi[1] and Haigun Lee[1]

Second-generation (2G) GdBCO-coated conductors (CCs) are promising for superconducting magnet applications because of their high critical current (I_c) density, low dependency of the I_c on the external magnetic field, good mechanical properties and reasonable cost, which offer opportunities to develop ultra-high-field magnets. However, they have not been used in high-temperature superconducting (HTS) applications with persistent current mode (PCM) operation such as nuclear magnetic resonance/magnetic resonance imaging magnets owing to unavailability of fabrication techniques for proper joining and contacts. Here we report a resistance-free joint, termed a 'superconducting joint', for 2G GdBCO CCs that forms a direct connection to establish a superconducting closed loop for PCM operation. The I_c value of the joined CCs is identical to that of the parent conductors in a liquid nitrogen bath (77 K). Moreover, the initially induced magnetic field of a model GdBCO coil containing a superconducting joint is maintained without decreasing, indicating the complete absence of electrical resistance. Thus, this fabrication method is a unique practical solution for lengthening the 2G HTS CCs and, more importantly, achieving PCM operation in 2G HTS magnet applications, including ultra-high-field nuclear magnetic resonance/magnetic resonance imaging magnets generating more than 1 GHz.

INTRODUCTION

Since the development of YBCO in 1987, the improvement of second-generation (2G) rare earth barium copper oxide-coated conductors (CCs) has been a triumph of scientific insight, sophisticated processing and determined scale-up efforts.[1–5] These CCs are promising for superconducting magnet applications because of their high I_c density, low dependency of the I_c on the external magnetic field, good mechanical properties and reasonable cost, which offer opportunities to develop ultra-high-field magnets.[6–8] Unfortunately, these CCs have not been used in superconducting devices with persistent current mode (PCM) operation such as magnets for magnetic resonance applications owing to the unavailability of fabrication techniques for proper joining and contacts.[9–12]

An ideal joint for 2G high-temperature superconducting (HTS) CCs requires perfect physical, chemical and mechanical continuity and uniformity throughout the CC-joint-CC connection, as well as sufficient metallurgical capacity without the formation of deleterious constituents, mechanical soundness and good performance under varying conditions, including closed-loop conditions for PCM operation. Various joining methods such as soldering are unsuitable for such joints because of their high joint resistance (20–2800 nΩ).[13,14] Accordingly, the physical continuity and uniformity necessary for obtaining a good I_c and electrical resistance have not

been achieved, precluding PCM operation. Hence, achieving superconducting joints for 2G HTS CCs that maintain the electrical characteristics of the parent CCs remains a challenge.[15,16]

Here, we report a 'superconducting joint' for 2G GdBCO CCs, that is, a direct connection between two superconducting layers formed without soldering that can establish a superconducting closed loop for PCM operation.

MATERIALS AND METHODS

Figure 1 shows the configuration of the GdBCO CC used in this study (SuperPower Inc., Schenectady, NY, USA). The width and overall thickness of the CC are 4 mm and 55 μm, respectively. The Ag stabilizer (∼2 μm) surrounded a Hastelloy substrate layer (50 μm), a buffer stack (0.2 μm) and a GdBCO layer (1 μm).

Producing the superconducting joint requires a series of processes, including fabrication of microholes by lasers, peeling off of the stabilizers, heat treatment for joining in vacuum and oxygenation annealing under high-pressure oxygen (Figure 2). In this process, the oxygen partial pressure (P_{O_2}) and temperature are the key parameters for ensuring thermodynamic stability of REBa$_2$Cu$_3$O$_{7-\delta}$ (RE123).[17,18]

For a direct GdBCO-GdBCO joint, an optimized etching method is necessary to eliminate the resistive stabilizers from the top of the GdBCO CC, because stabilizers between the two GdBCO CCs degrade conductivity. We used a chemical etching method to remove a predetermined length of the

[1]Department of Materials Science and Engineering, Korea University, Seoul, Republic of Korea and [2]KJoins Co. Ltd., Seoul, Republic of Korea
Correspondence: Professor HG Lee, Department of Materials Science and Engineering, Korea University, 145, Anam-dong, Seongbuk-gu, Seoul 136-713, Republic of Korea.
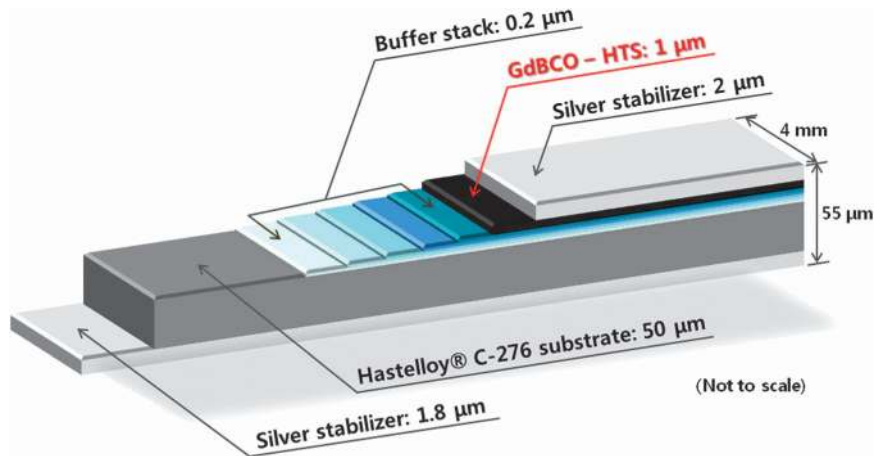E-mail: haigunlee@korea.ac.kr

Figure 1 Configuration of the GdBCO-coated conductors (CCs) used in this study (SuperPower).
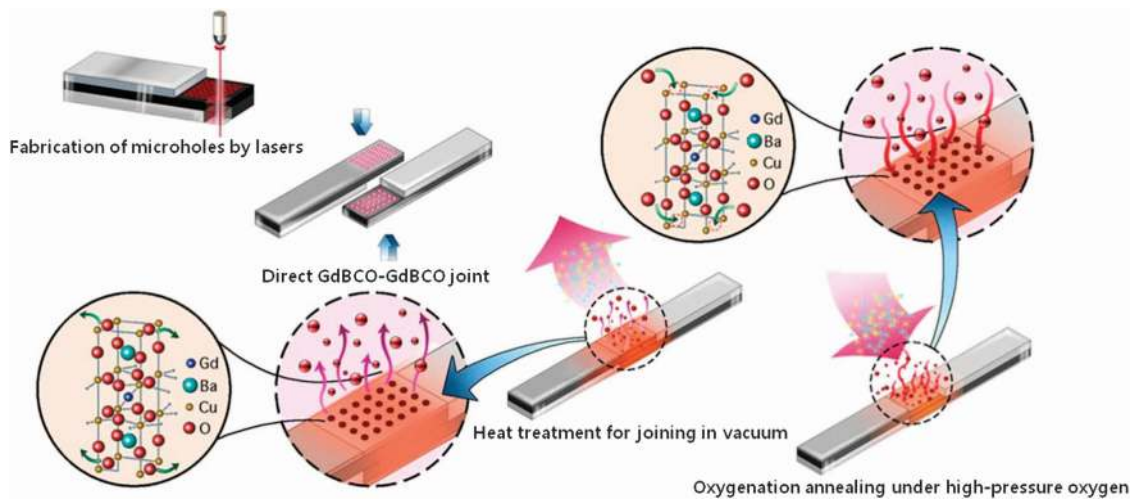

Figure 2 Procedures for fabricating a superconducting joint for GdBCO-coated conductors (CCs).

stabilizers covering the GdBCO to expose a portion of the bare GdBCO surface without degrading the superconductivity.[19–22] The ends of two bare GdBCO CCs are overlapped by rotating one CC 180° (to form a lap-type joint). The exposed portions of the superconducting layers are held together, and pressure is applied. The fixed portions of the superconducting layers are then heat-treated in the furnace under a reduced P_{O2} to melt-diffuse the superconducting layers in contact with each other.

During heat treatment, joining is achieved by atomic diffusion of the GdBCO with partial melting between the two GdBCO superconducting layers. The main parameters for joining are the heating rate, a peak temperature just above the peritectic temperature, the holding time at the peak temperature, the pressure applied to the joining region and the vacuum conditions of the furnace. The heating rate used is over 200 °C min^{-1} to minimize oxygen out-diffusion, and moderate cooling is applied after joining. The peak temperature of 850 °C is applied with pressures ~18 MPa on the joined region. The holding time at the peak temperature must be short, just barely enough for partial melting.[23,24] A reduced P_{O2} ($<10^{-2}$ Torr) is applied during splicing in the furnace, as the melting point of GdBCO decreases with decreasing P_{O2}. A low melting point decreases the oxygen out-diffusion from the GdBCO, which helps restore lost superconductivity. Furthermore, a successful superconducting joint can be obtained without melting the Ag stabilizer that protects the superconducting layer, because the melting point of GdBCO becomes lower than that of Ag at the reduced P_{O2}.[25]

The chemical reactions of GdBa$_2$Cu$_3$O$_{7-\delta}$ (Gd123) during heat treatment for joining are Gd123 → Gd123 + L(BaCuO$_2$ + CuO) → Gd211 + L(BaCuO$_2$ +

CuO), which can be summarized as GdBa$_2$Cu$_3$O$_{7-\delta}$ → 1/2[Gd$_2$BaCuO$_5$ + 3 BaCuO$_2$ + 2CuO + (0.5 + δ)O$_2$].[26,27] The reactions are irreversible, and the formation of Gd211, BaCuO$_2$ and CuO negatively affects the superconductivity. The ideal peak temperature should be below the threshold for the peritectic reaction [Gd123 → Gd123 + L(BaCuO$_2$ + CuO)] in order to induce diffusion bonding without forming Gd211, BaCuO$_2$ and CuO. However, rapid heating to just above the peritectic temperature is conducted because (1) two mirror-like faying surfaces for atomic diffusion are not achieved with two 1-μm-thick GdBCO layers and (2) partially melted liquid is required to increase the joint strength after solidification. In this process, portions of the joint after the heat treatment have compositions >98.26% Gd123, <0.93% Gd211, 0.78% BaCuO$_2$ and 0.03% CuO (Figure 3).

The superconducting layer is made from GdBa$_2$Cu$_3$O$_{7-\delta}$, in which the Gd:Ba:Cu molar ratio is 1:2:3 and the mole fraction (7−δ) of oxygen (O) typically ranged from 6.4 to 7. The structure and superconducting properties of GdBCO are strongly affected by the oxygen stoichiometry, and hence oxygen deficiencies cause a phase change from a superconducting orthorhombic phase to a non-superconducting tetragonal phase. This phase transition is dependent on the temperature and P_{O2}. Moreover, in an atmosphere containing oxygen, the phase transition is reversible under changes in temperature. However, it is irreversible in a vacuum, resulting in formation of a tetragonal phase that remains stable after heat treatment at high temperatures. Therefore, an oxygenation annealing process is performed to allow oxygen diffusion into
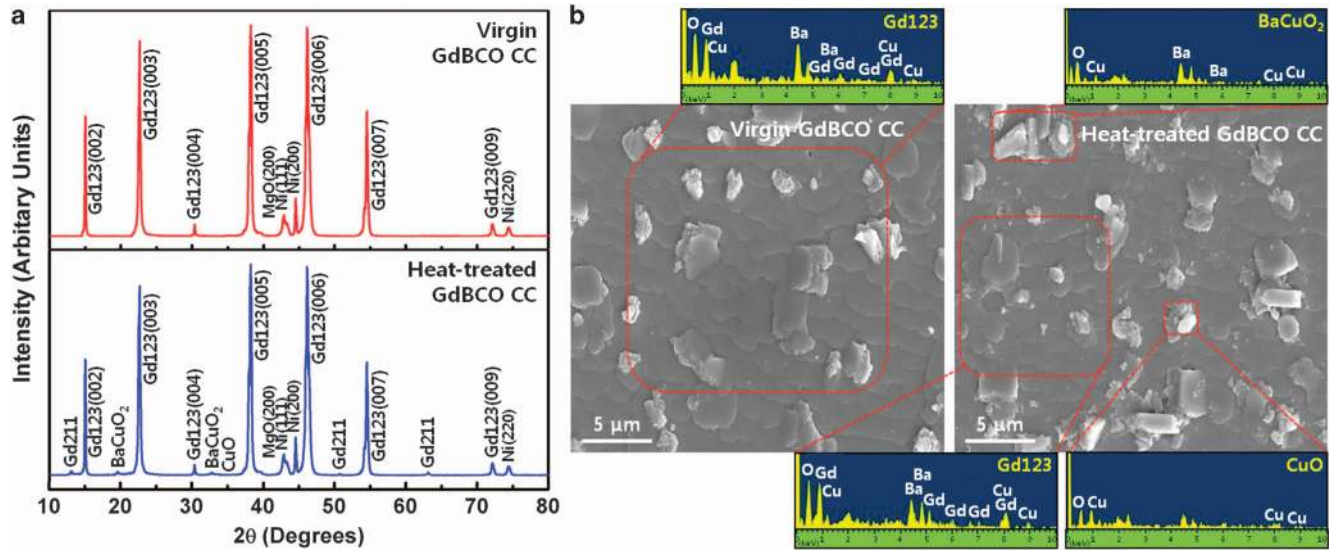
Figure 3 (**a**) X-ray diffraction (XRD) peaks of the heat-treated GdBCO-coated conductor (CC; at 850 °C and $P_{O2} < 10^{-2}$ Torr) correspond to the major XRD peaks (that is, Gd123 peaks) of the *c*-axis-oriented GdBCO peaks with few secondary phase products (such as BaCuO₂ and CuO) resulting from the partially melted GdBCO. (**b**) SEM image of the heat-treated GdBCO CC shows BaCuO₂ and CuO produced by decomposition of the GdBCO layer during the heat treatment, in contrast with the virgin GdBCO CC surface.
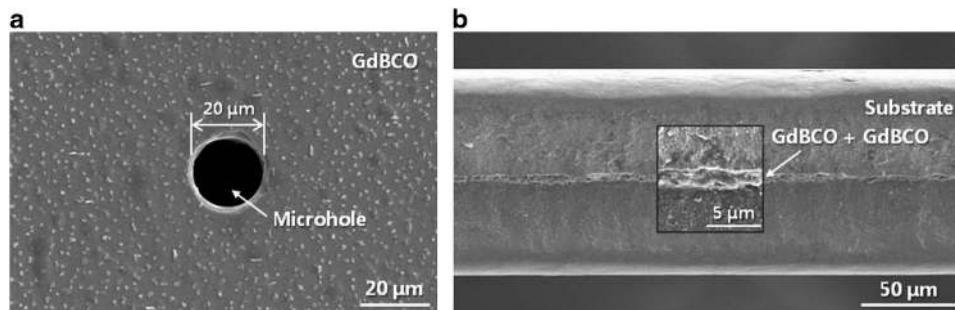

Figure 4 (**a**) SEM image of a microhole fabricated on the surface of the GdBCO-coated conductor (CC). (**b**) Cross-section of the joined region.

the oxygen-deficient lattices of GdBCO. An oxygen-rich environment restores the oxygen stoichiometry and hence the superconducting properties is lost during heat treatment.

The oxygenation annealing parameters are determined by the microstructural features affecting the diffusion process. To increase the oxygen content of GdBCO and restore its superconducting properties, oxygenation annealing is performed in an oxygen-rich environment ($P_{O2} = 5 \times 10^3$ Torr in 99.5% oxygen flow) at 500 °C, which is just below the orthorhombic-to-tetragonal transition temperature.[28] However, the superconductivity is only slightly recovered because of the low solubility and diffusivity of oxygen in the buffer and substrate materials of the GdBCO CCs. For successful oxygenation annealing of the joined CCs, it is essential to secure a diffusion path for oxygen in the joint region. Therefore, a laser drilling technique is used to produce microholes on the surface of the GdBCO CCs to act as conduits for oxygen. The holes penetrate through the substrates to facilitate oxygen diffusion to the GdBCO-joining area during oxygenation annealing. A large number of open pores in the microhole surfaces allow oxygen to reach the GdBCO lattice. The number and dimensions of the holes and the distance between them are optimized to achieve the highest I_c and index number (*n* value). In this study, the total number of microholes in the joining area (4×40 mm²) of each GdBCO CC is ~464. All layers of the CC (that is, substrate, buffer, superconducting and Ag stabilizer layers) are drilled, and the axial length of the microhole is 55 µm. The average diameter of the microhole is 20 µm (Figure 4a). The optimal oxygenation annealing parameters with respect to

microhole production on the CC surface to maximize atom rearrangement are 500 °C for 350 h with a heating rate of 10 °C min⁻¹ and a cooling rate of 0.5 °C min⁻¹.

RESULTS AND DISCUSSION

Figure 4b shows a typical SEM image of the GdBCO-joined area after the heat treatment and oxygenation annealing process. There are no cracks or large voids within the joined region and interface.

The self-field I_c values of the GdBCO CCs are measured in an LN₂ bath using a 1-µV cm⁻¹ criterion. Figure 5a shows the *V–I* curves of the virgin GdBCO CC and joined GdBCO CCs. The I_c value (84 A) of the joint is identical to that of the virgin CC, which indicates complete restoration of the superconducting property of the joint.

To determine the resistance, if any, of a GdBCO CC closed loop with a superconducting joint to a level below 10^{-12} Ω, the 'field-decay technique' is used.[29,30] In this technique, the time-dependent changes in a magnetic field generated by a current flowing in a circular loop containing an HTS joint are measured over many days. First, an Nd-Fe-B permanent magnet disk (0.35 T) is inserted into the GdBCO loop bore. When LN₂ is poured into the Styrofoam container, the GdBCO CC achieves superconductivity in the presence of the magnetic field induced by the Nd-Fe-B magnet (that is, field-
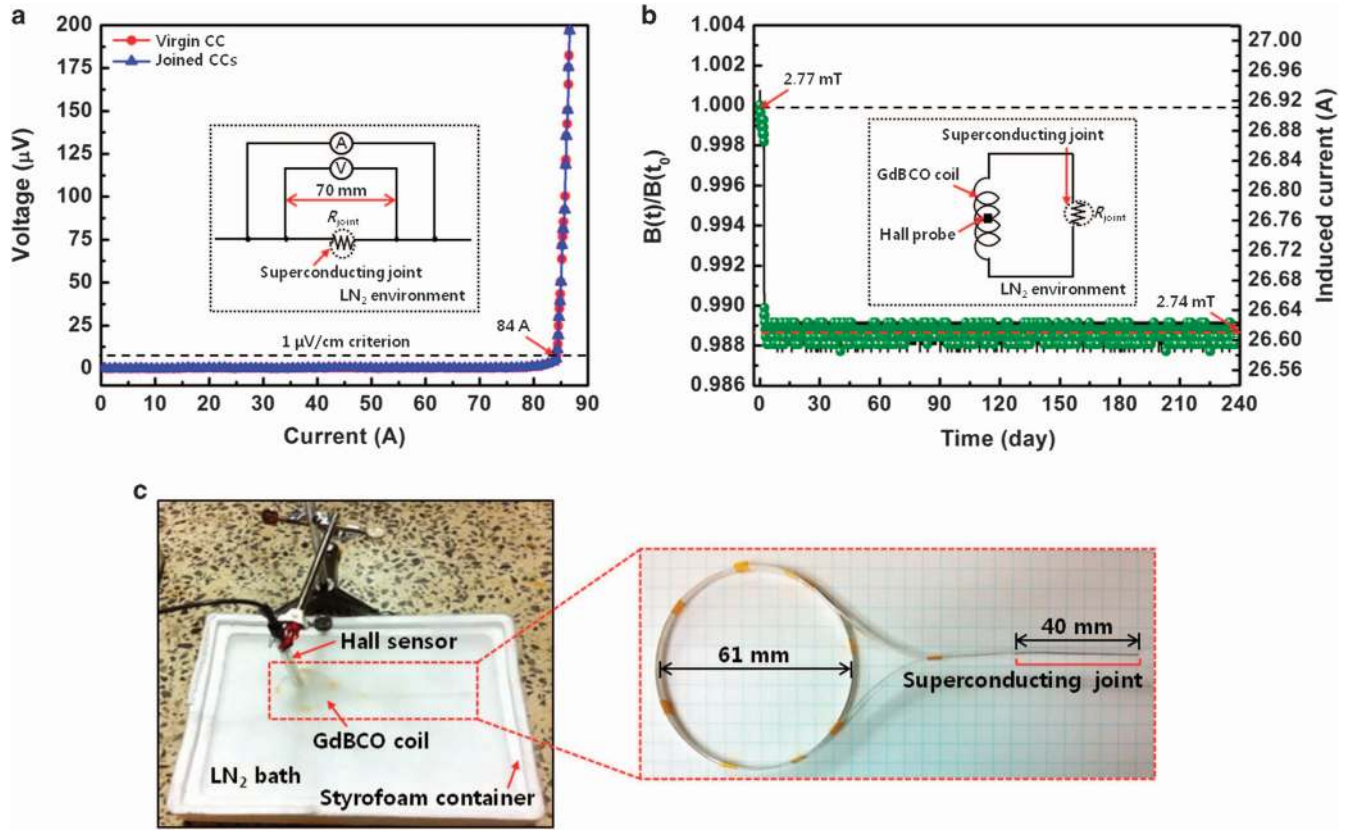
Figure 5 (**a**) The *V*–*I* curve of the joined GdBCO-coated conductors (CCs; blue line with triangles) is identical to that of the virgin GdBCO CC (red line with circles), indicating that the superconductivity after the joining process is perfectly recovered. The inset shows diagram of a standard four-point probe measurement structure. (**b**) Initial field of the GdBCO model coil fabricated with a superconducting joint that establishes a closed loop for persistent current mode (PCM) operation, which is maintained for 240 days. The inset shows diagram of a field-decay measurement structure. (**c**) Photographs of an actual field-decay measurement setup and a closed-loop GdBCO model coil. The diameter and joining length of the coil are 61 and 40 mm, respectively.

cooling occurred). After the permanent magnet is lifted out of the loop bore, a Hall sensor is placed at the center of the closed loop. The induced magnetic field on the GdBCO CC is measured by the Hall probe with an accuracy of 10^{-2} G and recorded with a data acquisition system.

Figure 5b shows the decay behavior of the induced field in the closed-loop GdBCO model coil fabricated using the developed joining method (Figure 5c). The vertical axis is normalized to the initial magnetic field. The field-decay rate of the GdBCO model coil is given by

$$B(t) = B(t_o)e^{-(R_{joint}/L)t}, \qquad (1)$$

where $B(t)$ is the induced magnetic field at t, $B(t_o)$ is the initially induced magnetic field, R_{joint} is the joint resistance, L is the self-inductance of a closed loop and t is time.

The initially induced magnetic field decays rapidly from 2.77 mT and reaches 2.74 mT 120 s after the current is induced by a field-cooling process. The initial field decay settles down to 2.74 mT, which corresponds to a superconducting current of 26.61 A, and subsequently remains steady for 240 days. Although the mechanisms of the rapid decay behavior in the early stage have been studied,[31,32] the decay behavior, especially in a HTS CC, has not been clearly understood. The initial decay of magnetic field may occur because the superconducting current induced by field cooling exceeds the capability of the superconducting layer and flows through the Ag

stabilizers.[33] In this study, the total circuit resistance at $L = 3.44 \, \mu$H is calculated using equation (1) as $< 10^{-17} \, \Omega$, which demonstrates that the model coil containing the superconducting joint operates in PCM.

Summary

In summary, the present work demonstrates the world's first super-conducting joint technique based on atomic diffusion in GdBCO with partial melting and oxygen diffusion into the oxygen-deficient GdBCO lattices. In the present case, unlike resistive splice, there is essentially no resistance to the flow of electricity between the CCs (perfect electrical connection). Our joining technique can resolve technical difficulties related to lengthening the 2G HTS CCs and, more importantly, the difficulty in establishing a superconducting closed loop for PCM operation. This method will provide unprecedented freedom to research scientists and development engineers in designing and manufacturing novel 2G HTS systems that would otherwise be impossible to produce using conventional 2G HTS splicing methods. Thus, the present technique will provide enormous benefits over conventional solutions to 2G HTS magnet applications in various areas, including energy (superconducting magnetic energy storage), alternative energy (wind turbine generators), medicine (nuclear magnetic resonance, magnetic resonance imaging), industry (motors, generators, magnetic separation, magnetic bearings), transportation (maglev, electric vehicle motors, commercial marine propulsion), military (electric ship propulsion, directed energy

weaponry, pulsed power systems), aerospace (space propulsion plasma rocket engine) and scientific research (high-energy physics, particle accelerators, synchrotron radiation).

CONFLICT OF INTEREST

The authors declare no conflict of interest.

1   Kang, S., Goyal, A., Li, J., Gapud, A. A., Martin, P. M., Heatherly, L., Thompson, J. R., Christen, D. K., List, F. A., Paranthaman, M. & Lee, D. F. High-performance high-T_c superconducting wires. *Science* **311,** 1911–1914 (2006).
2   Iwasa, Y. HTS magnets: stability; protection; cryogenics; economics; current stability/protection activities at FBML. *Cryogenics* **43,** 303–316 (2003).
3   Orenstein, J. & Millis, A. J. Advances in the physics of high-temperature superconductivity. *Science* **288,** 468–474 (2000).
4   Gutiérrez, J., Llordés, A., Gázquez, J., Gibert, M., Romà, N., Ricart, S., Pomar, A., Sandiumenge, F., Mestres, N., Puig, T. & Obradors, X. Strong isotropic flux pinning in solution-derived YBa$_2$Cu$_3$O$_{7-x}$ nanocomposite superconductor films. *Nat. Mater.* **6,** 367–373 (2007).
5   Selvamanickam, V., Chen, Y., Xiong, X., Xie, Y., Zhang, X., Rar, A., Martchevskii, M., Schmidt, R., Lenseth, K. & Herrin, J. Progress in second-generation HTS wire development and manufacturing. *Physica C* **468,** 1504–1509 (2008).
6   Larbalestier, D., Gurevich, A., Feldmann, D. M. & Polyanskii, A. High-T_c superconducting materials for electric power applications. *Nature* **414,** 368–377 (2001).
7   Hull, J. R. Applications of high-temperature superconductors in power technology. *Rep. Prog. Phys.* **66,** 1865–1886 (2003).
8   Lubkin, G. B. Power applications of high-temperature superconductors. *Phys. Today* **49,** 48 (1996).
9   Iliescu, S., Granados, X., Bartolomé, E., Sena, S., Carrillo, A. E., Puig, T., Obradors, X. & Evetts, J. E. High critical current YBa$_2$Cu$_3$O$_7$ artificial joints using Ag foils as welding agent. *Supercond. Sci. Technol.* **17,** 182–185 (2004).
10 Kato, J. Y., Sakai, N., Tajima, S., Miyata, S., Konishi, M., Yamada, Y., Chikumoto, N., Nakao, K., Izumi, T. & Shiohara, Y. Diffusion joint of YBCO coated conductors using stabilizing silver layers. *Physica C* **445–448,** 686–688 (2006).
11 Salama, K. & Selvamanickam, V. Joining of high current bulk Y-Ba-Cu-O superconductors. *Appl. Phys. Lett.* **60,** 898–900 (1992).
12 Sheahen, T. P. *Introduction to High-Temperature Superconductivity* 3–13 (Plenum Press, New York, 1994).
13 Kato, J. Y., Sakai, N., Tajima, S., Miyata, S., Watanabe, T., Yamada, Y., Chikumoto, N., Nakao, K., Izumi, T. & Shiohara, Y. Low resistance joint of the YBCO coated conductor. *J. Phys. Conf. Ser.* **43,** 166–169 (2006).
14 Park, D. K., Ahn, M. C., Kim, H. M., Lee, H. G., Chang, K. S., Lee, S. J., Yang, S. E. & Ko, T. K. Analysis of a joint method between superconducting YBCO coated conductors. *IEEE Trans. Appl. Supercond.* **17,** 3266–3269 (2007).
15 Selvamanickam, V., Chen, Y., Xiong, X., Xie, Y. Y., Reeves, J. L., Zhang, X., Qiao, Y., Lenseth, K. P., Schmidt, R. M., Rar, A., Hazelton, D. W. & Tekletsadik, K. Recent progress in second-generation HTS conductor scale-up at SuperPower. *IEEE Trans. Appl. Supercond.* **17,** 3231–3234 (2007).
16 Li, X., Rupich, M. W., Thieme, C. L. H., Teplitsky, M., Sathyamurthy, S., Thompson, E., Buczek, D., Schreiber, J., Demoranville, K., Lynch, J., Inch, J., Tucker, D., Savoy, R. & Fleshler, S. The development of second generation HTS wire at American Superconductor. *IEEE Trans. Appl. Supercond.* **19,** 3231–3235 (2009).
17 Park, Y. J., Shin, H. J., Kim, Y. G., Oh, Y. K. & Lee, H. G. Effects of melting diffusion and annealing in oxygen on superconducting characteristics of GdBCO coated conductors: Preliminary results. *IEEE Trans. Appl. Supercond.* **23,** 6600804 (2013).
18 Kim, H. S., Song, J. B., Kwon, N. Y., Kim, K. L. & Lee, H. G. The influence of heat-treatment and oxygenation annealing on the superconducting properties of YBCO coated conductors. *Supercond. Sci. Technol.* **22,** 125016 (2009).
19 Chang, K. S., Kim, H. K., Park, D. K., Ko, T. K., Ahn, M. C., Ha, D. H., Song, J. B., Lee, S. J., Kim, H. M. & Lee., H. G. Joint characteristics of YBCO coated conductor by removing a metallic stabilizer. *IEEE Trans. Appl. Supercond.* **18,** 1220–1223 (2008).
20 Kwon, N. Y., Kim, H. S., Kim, K. L., Yim, S. W., Kim, H. R., Hyun, O. B., Kim, H. M. & Lee, H. G. Influence of stabilizer thickness on over-current test of YBCO coated conductors (CC). *Supercond. Sci. Technol.* **22,** 045003 (2009).
21 Kim, H. S., Kwon, N. Y., Chang, K. S., Ko, T. K., Kim, H. M., Kim, W. S., Park, C. & Lee, H. G. Joint characteristics of the YBCO coated conductor (CC) by chemical etching. *IEEE Trans. Appl. Supercond.* **19,** 2835–2838 (2009).
22 Kwon, N. Y., Kim, H. S., Kim, K. L., Hahn, S. Y., Kim, H. R., Hyun, O. B., Kim, H. M., Kim, W. S., Park, C. & Lee, H. G. The effects of a stabilizer thickness of the YBCO coated conductor (CC) on the quench/recovery characteristics. *IEEE Trans. Appl. Supercond.* **20,** 1246–1249 (2010).
23 Chen, L., Claus, H., Paulikas, A. P., Zheng, H. & Veal, B. W. Joining of melt-textured YBCO: a direct contact method. *Supercond. Sci. Technol.* **15,** 672–674 (2002).
24 Lo, W. Recent progress in large-grain REBCO melt texturing. *JOM* **52,** 18–21 (2000).
25 Masuda, Y., Matsubara, K., Ogawa, R. & Kawate, Y. Production of YBa$_2$Cu$_3$O$_{7-x}$ thick films on Ag metal substrate controlled by oxygen. *Jpn J. Appl. Phys.* **31,** 2709–2715 (1992).
26 Aselagea, T. & Keefer, K. Liquidus relations in Y–Ba–Cu oxides. *J. Mater. Res.* **3,** 1279–1291 (1988).
27 Murakami, M. Processing of bulk YBaCuO. *Supercond. Sci. Technol.* **5,** 185–203 (1992).
28 Eatough, M. O., Ginley, D. S., Morosin, B. & Venturini, E. L. Orthorhombic-tetragonal phase transition in high-temperature superconductor YBa$_2$Cu$_3$O$_7$. *Appl. Phys. Lett.* **51,** 367–368 (1987).
29 Yao, W., Bascuñán, J., Hahn, S. Y. & Iwasa, Y. A superconducting joint technique for MgB$_2$ round wires. *IEEE Trans. Appl. Supercond.* **19,** 2261–2264 (2009).
30 Iwasa, Y. Superconducting joint between multifilamentary wires (Part II)-Joint evaluation technique. *Cryogenics* **16,** 217–219 (1976).
31 Han, Z., Vase, P., Shen, Y. Q. & Freltoft, T. Superconducting Bi$_2$Sr$_2$Ca$_2$Cu$_3$O$_x$ closed-loop coils carrying persistent current at temperatures above 77 K. *IEEE Trans. Appl. Supercond.* **7,** 873–876 (1997).
32 Horng, L. & Tai, C. H. Critical persistent current for a loop formed by a Bi-2223 Ag-sheathed superconducting tape. *IEEE Trans. Appl. Supercond.* **11,** 3006–3009 (2001).
33 Leupold, M. J. & Iwasa, Y. Superconducting joint between multifilamentary wires 1. Joint-making and joint results. *Cryogenics* **16,** 215–216 (1976).